
SVDinsTN: A Tensor Network Paradigm for Efficient Structure Search from Regularized Modeling Perspective

Yu-Bang Zheng¹, Xi-Le Zhao^{2,*}, Junhua Zeng^{3,4}, Chao Li⁴, Qibin Zhao⁴,
Heng-Chao Li¹, Ting-Zhu Huang²

¹School of Information Science and Technology, Southwest Jiaotong University

²School of Mathematical Sciences, University of Electronic Science and Technology of China

³School of Automation, Guangdong University of Technology

⁴Tensor Learning Team, RIKEN Center for Advanced Intelligence Project

*Corresponding author

Abstract

Tensor network (TN) representation is a powerful technique for computer vision and machine learning. TN structure search (TN-SS) aims to search for a customized structure to achieve a compact representation, which is a challenging NP-hard problem. Recent “sampling-evaluation”-based methods require sampling an extensive collection of structures and evaluating them one by one, resulting in prohibitively high computational costs. To address this issue, we propose a novel TN paradigm, named SVD-inspired TN decomposition (SVDinsTN), which allows us to efficiently solve the TN-SS problem from a regularized modeling perspective, eliminating the repeated structure evaluations. To be specific, by inserting a diagonal factor for each edge of the fully-connected TN, SVDinsTN allows us to calculate TN cores and diagonal factors simultaneously, with the factor sparsity revealing a compact TN structure. In theory, we prove a convergence guarantee for the proposed method. Experimental results demonstrate that the proposed method achieves approximately 100~1000 times acceleration compared to the state-of-the-art TN-SS methods while maintaining a comparable representation ability.

1 Introduction

Tensor network (TN) representation, which aims to express higher-order data with low-dimensional tensors (called TN cores) by a specific operation among them, has gained significant attention in various areas of data analysis [1, 23, 34], machine learning [4, 9], computer vision [19, 27, 32, 33], etc. By regarding TN cores as nodes and operations as edges, a TN corresponds to a graph (called TN topology). The vector composed of the weights of all edges in the topology is defined as the TN rank. *TN structure (including topology and rank) search (TN-SS)* aims to search for a suitable TN structure to achieve a compact representation for a given tensor, which is known as a challenging and theoretically NP-hard problem [12, 14]. The selection of TN structure dramatically impacts the performance of TN representation in practical applications [11, 13, 14].

Recently, there have been several notable efforts to tackle the TN-SS problem [11, 13, 14]. But most of them adopt the “sampling-evaluation” framework, which requires sampling a large number of structures as candidates and conducting numerous repeated structure evaluations. For instance, for a tensor of size $40 \times 60 \times 3 \times 9 \times 9$ (used in Section 4.2), TNGA in [13] requires *thousands* of evaluations and TNLE in [14] requires *hundreds* of evaluations, where each evaluation entails solving an optimization problem to compute TN cores iteratively. Consequently, the computational cost becomes exceedingly high. A meaningful question is *whether we can optimize the TN structure simultaneously during the computation*

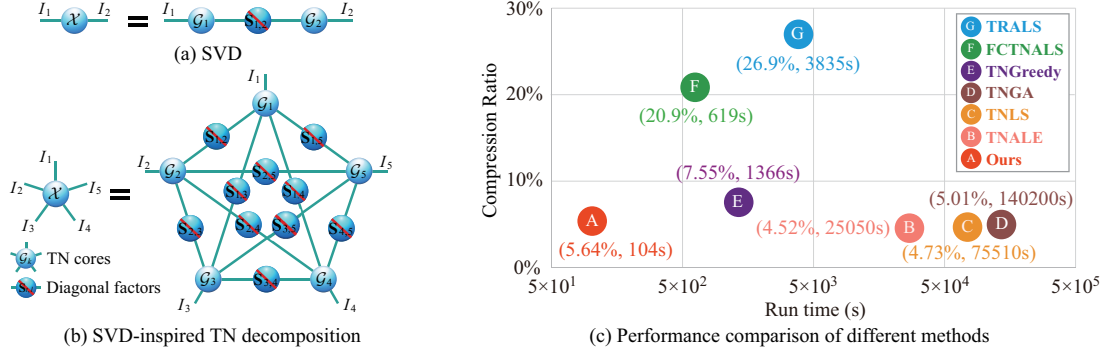


Figure 1: (a) A graphical illustration of SVD. (b) A graphical illustration of SVD-inspired TN decomposition on a fifth-order tensor. (c) Comparison of the compression ratio (\downarrow) and run time (\downarrow) of different methods on a fifth-order light field image *Knights*, where the reconstruction error bound is set to 0.05, TRALS [35] and FCTNALS [37] are methods with pre-defined topologies, and TNGreedy [11], TNGA [13], TNLS [15], and TNALE [14] are TN-SS methods (please see more results in Table 3).

of TN cores, thus escaping the “sampling-evaluation” framework and fundamentally addressing the computationally consuming issue.

In this paper, we introduce for the first time a regularized modeling perspective on solving the TN-SS problem. This perspective enables us to optimize the TN structure simultaneously during the computation of TN cores, effectively eliminating the need for repetitive structure evaluations. To be specific, we propose a novel TN paradigm, termed as *SVD-inspired TN decomposition (SVDinsTN)*, by inserting diagonal factors between any two TN cores in the “fully-connected” topology (see Figure 1(b)). *The intuition behind SVDinsTN is to leverage the sparsity of the inserted diagonal factors to reveal a compact TN structure and utilize the TN cores (merged with the diagonal factors) to represent a given tensor.* Based on SVDinsTN, we establish a regularized model, which updates the TN cores and diagonal factors iteratively and imposes a sparse operator to induce the sparsity of the diagonal factors. In theory, we prove a convergence guarantee for the proposed method and establish an upper bound for the TN rank. In particular, we design a novel initialization scheme for the proposed method based on the upper bound. This initialization scheme enables the proposed method to overcome the high computational cost in the first several iterations, which is caused by the utilization of a “fully-connected” topology as the starting point. As a result, SVDinsTN is capable of capturing a customized TN structure and providing a compact representation for a given tensor in an efficient manner. In summary, we make the following three contributions.

- We propose SVDinsTN, a new TN paradigm, that enables us to optimize the TN structure during the computation of TN cores, greatly reducing the computational cost.
- In theory, we prove a convergence guarantee for the proposed method and establish an upper bound for the TN rank involved in SVDinsTN. The upper bound serves as a guide for designing an efficient initialization scheme.
- Experimental results verify numerically that the proposed method achieves 100 ~ 1000 times acceleration compared to the state-of-the-art TN-SS methods with a comparable representation ability (see Figure 1(c)).

1.1 Related Works

TN representation¹ aims to find a set of small-sized TN cores to express a large-sized tensor under a TN structure (including topology and rank) [4, 5, 28]. In the past decades, many works focused on TN representation with a fixed TN topology, such as tensor train (TT) decomposition with a “chain” topology [22], tensor ring (TR) decomposition with a “ring” topology [35], fully-connected tensor network (FCTN) decomposition with a “fully-connected” topology [37], etc. In addition, these works also presented various methods to optimize the TN cores, such as alternating least square (ALS) [35], gradient descent (GD) [29, 31], proximal alternating minimization (PAM) [37], etc. In contrast, SVDinsTN can reveal

¹We primarily focus on TN representation in scientific computing and machine learning, while acknowledging its long history of research in physics [7, 21, 28].

Table 1: Several operations and their interpretations

Operation	Interpretation
diag	diag(\mathbf{X}) returns a column vector formed from the elements on the main diagonal of \mathbf{X} when the input variable is a diagonal matrix, and diag(\mathbf{x}) returns a diagonal matrix whose main diagonal is formed from the elements of \mathbf{x} when the input variable is a column vector.
ones	ones(I_1, I_2, \dots, I_N) returns an $I_1 \times I_2 \times \dots \times I_N$ tensor, whose elements are all equal to 1.
zeros	zeros(I_1, I_2, \dots, I_N) returns an $I_1 \times I_2 \times \dots \times I_N$ tensor, whose elements are all equal to 0.
vec	vec(\mathcal{X}) returns a column vector by lexicographical reordering of the elements of \mathcal{X} .

a compact TN structure for a given tensor, surpassing methods with pre-defined topologies in terms of representation ability.

TN structure search (TN-SS) aims to search for a suitable or optimal TN structure, including both topology and rank, to achieve a compact representation for a given tensor [8, 11, 13, 14, 15, 17, 18, 20, 24]. However, most existing TN-SS methods adopt the ‘‘sampling-evaluation’’ framework, making them require the utilization of heuristic search algorithms such as the greedy algorithm [11], genetic algorithm [13], and alternating local enumeration algorithm [14] to sample candidate structures and then evaluate them one by one. Therefore, these methods inevitably suffer from prohibitively high computational costs due to the numerous repeated evaluations, with each evaluation involving solving an optimization problem concerning the iterative calculation of TN cores. In contrast, SVDinsTN solves the TN-SS problem from a regularized modeling perspective, which avoids the repeated structure evaluations and greatly decreases the computational cost.

2 Notations and Preliminaries

We first summarize notations and several operations that will be used in the rest of the paper. Then, we review definitions related to tensor networks.

A *tensor* is a multi-dimensional array, and the number of dimensions (also called *modes*) of which is referred to as the *tensor order*. In the paper, first-order tensors (vectors), second-order tensors (matrices), and N th-order tensors are denoted by $\mathbf{x} \in \mathbb{R}^{I_1}$, $\mathbf{X} \in \mathbb{R}^{I_1 \times I_2}$, and $\mathcal{X} \in \mathbb{R}^{I_1 \times I_2 \times \dots \times I_N}$, respectively. We use $\|\mathcal{X}\|_F$ and $\|\mathcal{X}\|_1$ to denote the Frobenius norm and ℓ_1 -norm of \mathcal{X} , respectively. For brevity, we let \mathbb{K}_N denote the set $\{1, 2, \dots, N\}$, which is used for labeling individual indices. Similarly, we let $\mathbb{T}\mathbb{L}_N$ denote the set $\{(t, l) | 1 \leq t < l \leq N; t, l \in \mathbb{N}\}$, which is used for labeling paired indices.

We next provide a review of several operations on tensors [37].

The *generalized tensor unfolding* is an operation that converts a tensor into a matrix by merging a group of tensor modes into the rows of the matrix and merging the remaining modes into the columns. For example, an $I_1 \times I_2 \times I_3 \times I_4$ tensor can be unfolded into an $I_1 I_3 \times I_2 I_4$ matrix, denoted by $\mathbf{X}_{[1,3;2,4]}$. We use $\mathbf{X}_{[1,3;2,4]} = \text{GenUnfold}(\mathcal{X}, [1, 3; 2, 4])$ and $\mathcal{X} = \text{GenFold}(\mathbf{X}_{[1,3;2,4]}, [1, 3; 2, 4])$ to simply denote the corresponding operation and inverse operation, respectively. We also use $\mathbf{X}_{(2)}$ to simply represent $\mathbf{X}_{[2;1,3,4]} \in \mathbb{R}^{I_2 \times I_1 I_3 I_4}$, which is also called *mode-2 unfolding*. Besides, we use $\mathbf{X}_{(2)} = \text{Unfold}(\mathcal{X}, 2)$ and $\mathcal{X} = \text{Fold}(\mathbf{X}_{(2)}, 2)$ to simply denote the corresponding operation and inverse operation, respectively.

The *generalized tensor transposition* is an operation that rearranges tensor modes in the order specified by a vector. For example, an $I_1 \times I_2 \times I_3 \times I_4$ tensor can be transposed into an $I_3 \times I_2 \times I_1 \times I_4$ tensor, denoted by $\vec{\mathcal{X}}^{\mathbf{n}}$ with $\mathbf{n} = (3, 2, 1, 4)$. We use $\vec{\mathcal{X}}^{\mathbf{n}} = \text{permute}(\mathcal{X}, \mathbf{n})$ and $\mathcal{X} = \text{ipermute}(\vec{\mathcal{X}}^{\mathbf{n}}, \mathbf{n})$ to simply denote the corresponding operation and inverse operation, respectively.

The *tensor contraction* is an operation that obtains a new tensor by pairing, multiplying, and summing indices of certain modes of two tensors. For example, if a fourth-order tensor $\mathcal{X} \in \mathbb{R}^{I_1 \times I_2 \times I_3 \times I_4}$ and a third-order tensor $\mathcal{Y} \in \mathbb{R}^{J_1 \times J_2 \times J_3}$ satisfy $I_2 = J_1$ and $I_4 = J_2$, then the tensor contraction between the 2nd and 4th modes of \mathcal{X} and the 1st and 2nd modes of \mathcal{Y} yields a tensor $\mathcal{Z} = \mathcal{X} \times_{2,4}^{1,2} \mathcal{Y} \in \mathbb{R}^{I_1 \times I_3 \times J_3}$. The elements of \mathcal{Z} are calculated as follows:

$$\mathcal{Z}(i_1, i_3, j_3) = \sum_{i_2=1}^{I_2} \sum_{i_4=1}^{I_4} \mathcal{X}(i_1, i_2, i_3, i_4) \mathcal{Y}(i_2, i_4, j_3).$$

In Table 1, we give the interpretations of the operations ‘‘diag’’, ‘‘ones’’, ‘‘zeros’’, and ‘‘vec’’.

2.1 Tensor Network

In general, a *tensor network (TN)* is defined as a collection of low-dimensional tensors, known as TN cores, in which some or all modes are contracted according to specific operations [4]. The primary purpose of a TN is to represent higher-order data using these TN cores. By considering TN cores as nodes and operations between modes of cores as edges, we define the graph formed by these nodes and edges as the TN topology. Additionally, we assign a non-negative integer weight to each edge to indicate the size of the corresponding TN core, and call the vector composed of these edge weights the TN rank. Consequently, a TN structure refers to a weighted graph comprising nodes, edges, and weights, encompassing both the TN topology and TN rank.

This paper focuses on only a class of TNs that employs tensor contraction as the operation among TN cores and adopts a simple graph as the TN topology. More particularly, when representing an N th-order tensor \mathcal{X} , this class of TNs comprises precisely N TN cores, each corresponding to one mode of \mathcal{X} . A notable method is the FCTN decomposition, which represents an N th-order tensor $\mathcal{X} \in \mathbb{R}^{I_1 \times I_2 \times \dots \times I_N}$ by N small-sized N th-order cores denoted by $\mathcal{G}_k \in \mathbb{R}^{R_{1,k} \times R_{2,k} \times \dots \times R_{k-1,k} \times I_k \times R_{k,k+1} \times \dots \times R_{k,N}}$ for $k \in \mathbb{K}_N$ [37]. In this decomposition, any two cores \mathcal{G}_l and \mathcal{G}_t for $(t, l) \in \mathbb{T}\mathbb{L}_N$ share an equal-sized mode $R_{t,l}$ used for tensor contraction. We denote the FCTN decomposition by $\mathcal{X} = \text{FCTN}(\mathcal{G}_1, \mathcal{G}_2, \dots, \mathcal{G}_N)$ and define the FCTN rank as the vector $(R_{1,2}, R_{1,3}, \dots, R_{1,N}, R_{2,3}, \dots, R_{2,N}, \dots, R_{N-1,N}) \in \mathbb{R}^{N(N-1)/2}$. According to the concept of tensor contraction, removing rank-one edges in the TN topology does not change the expression of the TN. This means that if any element in the FCTN rank is equal to one, the corresponding edge can be harmlessly eliminated from the “fully-connected” topology. For instance, a “fully-connected” topology with the rank $(R_{1,2}, 1, \dots, 1, R_{2,3}, 1, \dots, 1, R_{N-2,N-1}, R_{N-1,N})$ can be converted into a “chain” topology with rank $(R_{1,2}, R_{2,3}, \dots, R_{N-1,N})$ in this manner. This fact can be formally stated as follows.

Property 1 [16] There exists a one-to-one correspondence between the *TN structure* and *FCTN rank*.

This work is inspired by Property 1, searching for a more compact TN structure by optimizing the FCTN rank.

3 An Efficient Method for TN-SS

We propose an efficient method to solve the TN-SS problem from a regularized modeling perspective. Unlike the existing “sampling-evaluation” framework, the *main idea* of the proposed method is to optimize the TN structure simultaneously during the computation of TN cores, thereby eliminating the need for repetitive structure evaluations and greatly decreasing the computational cost.

3.1 SVDinsTN

We start with the definition of the following SVDinsTN.

Definition 1 (SVDinsTN) Let $\mathcal{X} \in \mathbb{R}^{I_1 \times I_2 \times \dots \times I_N}$ be an N th-order tensor such that

$$\begin{aligned} \mathcal{X}(i_1, i_2, \dots, i_N) = & \sum_{r_{1,2}=1}^{R_{1,2}} \sum_{r_{1,3}=1}^{R_{1,3}} \dots \sum_{r_{1,N}=1}^{R_{1,N}} \sum_{r_{2,3}=1}^{R_{2,3}} \dots \sum_{r_{2,N}=1}^{R_{2,N}} \dots \sum_{r_{N-1,N}=1}^{R_{N-1,N}} \\ & \mathbf{S}_{1,2}(r_{1,2}, r_{1,2}) \mathbf{S}_{1,3}(r_{1,3}, r_{1,3}) \dots \mathbf{S}_{1,N}(r_{1,N}, r_{1,N}) \\ & \mathbf{S}_{2,3}(r_{2,3}, r_{2,3}) \dots \mathbf{S}_{2,N}(r_{2,N}, r_{2,N}) \dots \\ & \mathbf{S}_{N-1,N}(r_{N-1,N}, r_{N-1,N}) \\ & \mathcal{G}_1(i_1, r_{1,2}, r_{1,3}, \dots, r_{1,N}) \\ & \mathcal{G}_2(r_{1,2}, i_2, r_{2,3}, \dots, r_{2,N}) \dots \\ & \mathcal{G}_k(r_{1,k}, r_{2,k}, \dots, r_{k-1,k}, i_k, r_{k,k+1}, \dots, r_{k,N}) \dots \\ & \mathcal{G}_N(r_{1,N}, r_{2,N}, \dots, r_{N-1,N}, i_N), \end{aligned} \quad (1)$$

where $\mathcal{G}_k \in \mathbb{R}^{R_{1,k} \times R_{2,k} \times \dots \times R_{k-1,k} \times I_k \times R_{k,k+1} \times \dots \times R_{k,N}}$ for $\forall k \in \mathbb{K}_N$ are N th-order tensors and called TN cores, and $\mathbf{S}_{t,l} \in \mathbb{R}^{R_{t,l} \times R_{t,l}}$ for $\forall (t, l) \in \mathbb{T}\mathbb{L}_N$ are diagonal matrices. Then we call (1) an SVD-inspired TN decomposition (SVDinsTN) of \mathcal{X} , denoted by $\mathcal{X} = \text{STN}(\mathcal{G}, \mathbf{S})$, where \mathcal{G} denotes $\{\mathcal{G}_k | k \in \mathbb{K}_N\}$ and \mathbf{S} denotes $\{\mathbf{S}_{t,l} | (t, l) \in \mathbb{T}\mathbb{L}_N\}$.

Figure 1(b) shows a graphical illustration of SVDinsTN on a fifth-order tensor. SVDinsTN includes TN cores and diagonal factors, enables it to leverage the sparsity of diagonal factors to reveal a compact TN structure and utilize TN cores (merged with diagonal factors) to represent a tensor.

Remark 1 (SVDinsTN & SVD) *SVDinsTN extends upon the “core&diagonal factor&core” form of SVD to higher-order cases (see Figure 1(a) & (b)), incorporating the idea of determining rank through non-zero elements in the diagonal factor. In particular, SVDinsTN can degrade into SVD in second-order cases (matrices) when TN cores satisfy orthogonality.*

Remark 2 (SVDinsTN & FCTN) *SVDinsTN builds upon FCTN decomposition [37] but can reveal the FCTN rank (TN structure). It achieves this by inserting diagonal factors between any two TN cores in FCTN decomposition and leveraging the number of non-zero elements in the diagonal factors to determine the FCTN rank. In particular, SVDinsTN can transform into a TN (includes but is not limited to FCTN) decomposition by merging the diagonal factors into TN cores through the tensor contraction operation.*

3.2 A Regularized Method for TN-SS

We present an SVDinsTN-based regularized method, which updates TN cores and diagonal factors simultaneously, and imposes a sparse operator to induce the sparsity of diagonal factors to reveal a compact TN structure.

We consider an ℓ_1 -norm-based operator for diagonal factors \mathbf{S} and Tikhonov regularization [10] for TN cores \mathcal{G} . The ℓ_1 -norm-based operator is used to promote the sparsity of \mathbf{S} , and the Tikhonov regularization is used to constrict the feasible range of \mathcal{G} . Mathematically, the proposed model can be formulated as follows:

$$\min_{\mathcal{G}, \mathbf{S}} \frac{1}{2} \|\mathcal{X} - \text{STN}(\mathcal{G}, \mathbf{S})\|_F^2 + \frac{\mu}{2} \sum_{k \in \mathbb{K}_N} \|\mathcal{G}_k\|_F^2 + \sum_{(t,l) \in \mathbb{TL}_N} \lambda_{t,l} \|\mathbf{S}_{t,l}\|_1, \quad (2)$$

where $\lambda_{t,l} > 0$ for $\forall (t,l) \in \mathbb{TL}_N$ and $\mu > 0$ are regularization parameters, \mathcal{G} denotes $\{\mathcal{G}_k | k \in \mathbb{K}_N\}$, and \mathbf{S} denotes $\{\mathbf{S}_{t,l} | (t,l) \in \mathbb{TL}_N\}$.

We use the PAM-based algorithm [2] to solve (2), whose solution is obtained by alternately updating

$$\begin{cases} \mathcal{G}_k = \underset{\mathcal{G}_k}{\operatorname{argmin}} \frac{1}{2} \|\mathcal{X} - \text{STN}(\mathcal{G}, \mathbf{S})\|_F^2 + \frac{\mu}{2} \|\mathcal{G}_k\|_F^2 + \frac{\rho}{2} \|\mathcal{G}_k - \hat{\mathcal{G}}_k\|_F^2, \forall k \in \mathbb{K}_N, \\ \mathbf{S}_{t,l} = \underset{\mathbf{S}_{t,l}}{\operatorname{argmin}} \frac{1}{2} \|\mathcal{X} - \text{STN}(\mathcal{G}, \mathbf{S})\|_F^2 + \lambda_{t,l} \|\mathbf{S}_{t,l}\|_1 + \frac{\rho}{2} \|\mathbf{S}_{t,l} - \hat{\mathbf{S}}_{t,l}\|_F^2, \forall (t,l) \in \mathbb{TL}_N, \end{cases} \quad (3)$$

where $\rho > 0$ is a proximal parameter (we fix $\rho = 0.001$), and $\hat{\mathcal{G}}_k$ and $\hat{\mathbf{S}}_{t,l}$ are the solutions of the \mathcal{G}_k -subproblem and $\mathbf{S}_{t,l}$ -subproblem at the previous iteration, respectively.

1) *Update \mathcal{G}_k for $\forall k \in \mathbb{K}_N$:* Solving the \mathcal{G}_k -subproblem requires fixing the other TN cores and diagonal factors. To address this, we use \mathbf{M}_k to denote the matrix obtained by performing tensor contraction and unfolding operations on all diagonal factors and TN cores except \mathcal{G}_k . Algorithm 1 presents a way to compute \mathbf{M}_k . We can obtain $\mathbf{X}_{(k)} = \mathbf{G}_{k(k)} \mathbf{M}_k$. In this way, the \mathcal{G}_k -subproblem can be rewritten as follows:

$$\min_{\mathbf{G}_{k(k)}} \frac{1}{2} \|\mathbf{X}_{(k)} - \mathbf{G}_{k(k)} \mathbf{M}_k\|_F^2 + \frac{\mu}{2} \|\mathbf{G}_{k(k)}\|_F^2 + \frac{\rho}{2} \|\mathbf{G}_{k(k)} - \hat{\mathbf{G}}_{k(k)}\|_F^2. \quad (4)$$

The objective function of (4) is differentiable, and thus its solution can be obtained by

$$\mathbf{G}_{k(k)} = (\mathbf{X}_{(k)} \mathbf{M}_k^T + \rho \hat{\mathbf{G}}_{k(k)}) (\mathbf{M}_k \mathbf{M}_k^T + (\mu + \rho) \mathbf{I})^{-1}. \quad (5)$$

2) *Update $\mathbf{S}_{t,l}$ for $\forall (t,l) \in \mathbb{TL}_N$:* Solving the $\mathbf{S}_{t,l}$ -subproblem requires fixing the other diagonal factors and TN cores. In a similar fashion, we use $\mathbf{H}_{t,l}$ to denote the matrix obtained by performing tensor contraction and unfolding operations on all TN cores and diagonal factors except $\mathbf{S}_{t,l}$. Algorithm 2 presents a way to compute $\mathbf{H}_{t,l}$. We can obtain $\mathbf{x} = \mathbf{H}_{t,l} \mathbf{s}_{t,l}$, where $\mathbf{x} = \operatorname{vec}(\mathcal{X})$ and $\mathbf{s}_{t,l} = \operatorname{diag}(\mathbf{S}_{t,l})$. In this way, the $\mathbf{S}_{t,l}$ -subproblem can be rewritten as follows:

$$\min_{\mathbf{s}_{t,l}} \frac{1}{2} \|\mathbf{x} - \mathbf{H}_{t,l} \mathbf{s}_{t,l}\|_F^2 + \lambda_{t,l} \|\mathbf{s}_{t,l}\|_1 + \frac{\rho}{2} \|\mathbf{s}_{t,l} - \hat{\mathbf{s}}_{t,l}\|_F^2. \quad (6)$$

Algorithm 1 $\mathbf{M}_k = \text{STN}(\{\mathcal{G}_q\}_{q=1}^N, \{\mathbf{S}_{t,l}\}_{1 \leq t < l \leq N}^{t,l \in \mathbb{N}} / \mathcal{G}_k)$.

Input: $\mathcal{G}_q \in \mathbb{R}^{R_{1,q} \times R_{2,q} \times \dots \times R_{q-1,q} \times I_q \times R_{q,q+1} \times \dots \times R_{q,N}}$ for $q = 1, 2, \dots, k-1, k+1, \dots, N$; $\mathbf{S}_{t,l} \in \mathbb{R}^{R_{t,l} \times R_{t,l}}$ for $1 \leq t < l \leq N$ and $t, l \in \mathbb{N}$; and $k \in \{1, 2, \dots, N\}$.

Initialization: $\mathbf{a} = (k+1 : N, 1 : k)$.

```

1: for  $i = 1$  to  $k-1$  and  $i = k+1$  to  $N-1$  do
2:   for  $j = i+1$  to  $N$  do
3:     Let  $\mathcal{G}_i = \mathcal{G}_i \times_{i+1}^1 \mathbf{S}_{i,j}$ .
4:   end for
5:   if  $i > k$  then
6:     Let  $\mathcal{G}_i = \mathcal{G}_i \times_k^1 \mathbf{S}_{k,i}$ .
7:     Let  $\mathcal{G}_i = \text{permute}(\mathcal{G}_i, (1 : k-1, N, k : N-1))$ .
8:   end if
9:   Let  $\mathcal{G}_i = \text{permute}(\mathcal{G}_i, \mathbf{a})$ .
10: end for
11: Let  $\mathcal{M}_k = \mathcal{G}_{\mathbf{a}(1)}$ ,  $m_1 = 1$ , and  $n_1 = 2$ .
12: for  $i = 1$  to  $N-2$  do
13:   Let  $\mathcal{M}_k = \mathcal{M}_k \times_{n_1, n_2, \dots, n_i}^{m_1, m_2, \dots, m_i} \mathcal{G}_{\mathbf{a}(i+1)}$ .
14:   Let  $m_j = j$  for  $j = 1, 2, \dots, i+1$ .
15:   Let  $n_j = 2 + (j-1)(N-i)$  for  $j = 1, 2, \dots, i+1$ .
16: end for
17: Let  $\mathcal{M}_k = \text{permute}(\mathcal{M}_k, (2(N-k)+1 : 2(N-1), 1 : 2(N-k)))$ .
18: Let  $\mathbf{c} = \text{zeros}(1, N-1)$  and  $\mathbf{d} = \text{zeros}(1, N-1)$ .
19: for  $i = 1$  to  $N-1$  do
20:   Let  $\mathbf{c}(i) = 2i$  and  $\mathbf{d}(i) = 2i-1$ .
21: end for
22: Let  $\mathbf{M}_k = \text{GenUnfold}(\mathcal{M}_k, [\mathbf{c}; \mathbf{d}])$ .

```

Output: The matrix $\mathbf{M}_k \in \mathbb{R}^{\prod_{i=1}^{k-1} R_{i,k} \prod_{i=k+1}^N R_{k,i} \times \prod_{i=1, i \neq k}^N I_i}$.

We use an alternating direction method of multipliers (ADMM) [6] to solve (6) and rewrite it as follows:

$$\begin{aligned} \min_{\mathbf{s}_{t,l}} \quad & \frac{1}{2} \|\mathbf{x} - \mathbf{H}_{t,l} \mathbf{q}_{t,l}\|_F^2 + \lambda_{t,l} \|\mathbf{s}_{t,l}\|_1 + \frac{\rho}{2} \|\mathbf{s}_{t,l} - \hat{\mathbf{s}}_{t,l}\|_F^2 \\ \text{s.t.} \quad & \mathbf{s}_{t,l} - \mathbf{q}_{t,l} = 0, \end{aligned} \quad (7)$$

where $\mathbf{q}_{t,l}$ is a auxiliary variable. The augmented Lagrangian function of (7) can be expressed as the following concise form:

$$\begin{aligned} L_{\beta_{t,l}}(\mathbf{s}_{t,l}, \mathbf{q}_{t,l}, \mathbf{p}_{t,l}) = & \frac{1}{2} \|\mathbf{x} - \mathbf{H}_{t,l} \mathbf{q}_{t,l}\|_F^2 + \lambda_{t,l} \|\mathbf{s}_{t,l}\|_1 \\ & + \frac{\rho}{2} \|\mathbf{s}_{t,l} - \hat{\mathbf{s}}_{t,l}\|_F^2 + \frac{\beta_{t,l}}{2} \left\| \mathbf{s}_{t,l} - \mathbf{q}_{t,l} + \frac{\mathbf{p}_{t,l}}{\beta_{t,l}} \right\|_F^2, \end{aligned} \quad (8)$$

where $\mathbf{p}_{t,l}$ is the Lagrangian multiplier and $\beta_{t,l}$ is the penalty parameter. Within the ADMM framework, $\mathbf{q}_{t,l}$, $\mathbf{s}_{t,l}$, and $\mathbf{p}_{t,l}$ can be solved by alternately updating

$$\begin{cases} \mathbf{q}_{t,l} = \underset{\mathbf{q}_{t,l}}{\text{argmin}} \quad \frac{1}{2} \|\mathbf{x} - \mathbf{H}_{t,l} \mathbf{q}_{t,l}\|_F^2 + \frac{\beta_{t,l}}{2} \left\| \mathbf{s}_{t,l} - \mathbf{q}_{t,l} + \frac{\mathbf{p}_{t,l}}{\beta_{t,l}} \right\|_F^2, \\ \mathbf{s}_{t,l} = \underset{\mathbf{s}_{t,l}}{\text{argmin}} \quad \lambda_{t,l} \|\mathbf{s}_{t,l}\|_1 + \frac{\rho}{2} \|\mathbf{s}_{t,l} - \hat{\mathbf{s}}_{t,l}\|_F^2 + \frac{\beta_{t,l}}{2} \left\| \mathbf{s}_{t,l} - \mathbf{q}_{t,l} + \frac{\mathbf{p}_{t,l}}{\beta_{t,l}} \right\|_F^2, \\ \mathbf{p}_{t,l} = \mathbf{p}_{t,l} + \beta_{t,l} (\mathbf{s}_{t,l} - \mathbf{q}_{t,l}). \end{cases} \quad (9)$$

That is,

$$\begin{cases} \mathbf{q}_{t,l} = [\mathbf{H}_{t,l}^T \mathbf{H}_{t,l} + \beta_{t,l} \mathbf{I}]^{-1} [\mathbf{H}_{t,l}^T \mathbf{x} + \beta_{t,l} \mathbf{s}_{t,l} + \mathbf{p}_{t,l}], \\ \mathbf{s}_{t,l} = \text{shrink} \left(\frac{\rho \hat{\mathbf{s}}_{t,l} + \beta_{t,l} \mathbf{q}_{t,l} - \mathbf{p}_{t,l}}{\rho + \beta_{t,l}}, \frac{\lambda_{t,l}}{\rho + \beta_{t,l}} \right), \\ \mathbf{p}_{t,l} = \mathbf{p}_{t,l} + \beta_{t,l} (\mathbf{s}_{t,l} - \mathbf{q}_{t,l}), \end{cases} \quad (10)$$

where $\text{shrink}(\mathbf{a}, \mathbf{b}) = \max(\mathbf{a} - \mathbf{b}, \mathbf{0}) + \min(\mathbf{a} + \mathbf{b}, \mathbf{0})$.

Algorithm 2 $\mathbf{H}_{t,l} = \text{STN}(\{\mathcal{G}_k\}_{k=1}^N, \{\mathbf{S}_{p,q}\}_{1 \leq p < q \leq N}^{p,q \in \mathbb{N}}, / \mathbf{S}_{t,l})$.

Input: $\mathcal{G}_k \in \mathbb{R}^{R_{1,k} \times R_{2,k} \times \dots \times R_{k-1,k} \times I_k \times R_{k,k+1} \times \dots \times R_{k,N}}$ for $k = 1, 2, \dots, N$; $\mathbf{S}_{p,q} \in \mathbb{R}^{R_{p,q} \times R_{p,q}}$ for $1 \leq p < q \leq N$, $p, q \in \mathbb{N}$, and $(p, q) \neq (t, l)$; and $t \in \{1, 2, \dots, N\}$ and $l \in \{t+1, t+2, \dots, N\}$.

```

1: for  $i = 1$  to  $t-1$  and  $i = t+1$  to  $N-1$  do
2:   for  $j = i+1$  to  $N$  do
3:     Let  $\mathcal{G}_i = \mathcal{G}_i \times_{i+1}^1 \mathbf{S}_{i,j}$ .
4:   end for
5: end for
6: for  $j = t+1$  to  $l-1$  do
7:   Let  $\mathcal{G}_t = \mathcal{G}_t \times_{t+1}^1 \mathbf{S}_{t,j}$ .
8: end for
9: for  $j = l+1$  to  $N$  do
10:  Let  $\mathcal{G}_t = \mathcal{G}_t \times_{t+2}^1 \mathbf{S}_{t,j}$ .
11: end for
12: Let  $\mathcal{G}_t = \text{permute}(\mathcal{G}_t, (1 : t, t+2 : l, t+1, l+1 : N))$ .
13: Let  $\mathbf{G}_t = \text{Unfold}(\mathcal{G}_t, l)$  and  $\mathbf{G}_l = \text{Unfold}(\mathcal{G}_l, t)$ .
14: Let  $\mathbf{H}_{t,l} = \text{zeros}(\prod_{k=1}^N I_k, R_{t,l})$ .
15: for  $i = 1$  to  $R_{t,l}$  do
16:   Let  $\mathcal{G}_t = \text{Fold}(\mathbf{G}_t(i, :), l)$  and  $\mathcal{G}_l = \text{Fold}(\mathbf{G}_l(i, :), t)$ .
17:   Let  $\mathbf{H}_{t,l}(:, i) = \text{vec}(\text{FCTN}(\{\mathcal{G}_k\}_{k=1}^N))$ .
18: end for

```

Output: The matrix $\mathbf{H}_{t,l} \in \mathbb{R}^{\prod_{k=1}^N I_k \times R_{t,l}}$.

Algorithm 3 PAM-based algorithm to optimize model (2).

Input: A tensor $\mathcal{X} \in \mathbb{R}^{I_1 \times I_2 \times \dots \times I_N}$ and a parameter γ .

Initialization: Initialize $\mathbf{S}_{t,l}$ and $R_{t,l}$ by the initialization scheme in Section 3.3 and let $\beta_{t,l} = 1$ for $\forall (t, l) \in \mathbb{TL}_N$;
 let $\mathcal{G}_k = 1/\sqrt{I_k}$ ones($R_{1,k}, R_{2,k}, \dots, R_{k-1,k}, I_k, R_{k,k+1}, \dots, R_{k,N}$) for $\forall k \in \mathbb{K}_N$ and $\mu = 1$.

```

1: while not converged do
2:   Let  $\tilde{\mathcal{X}} = \mathcal{X}$  and  $\lambda_{t,l} = \gamma \max(\mathbf{S}_{t,l})(\rho + \beta_{t,l})$ .
3:   Update  $\mathcal{G}_k$  by (5) and let  $\mathcal{G}_k = \text{Fold}(\mathbf{G}_{k(k)}, k)$ .
4:   for  $i = 1$  to 5 do
5:     Update  $\mathbf{q}_{t,l}$ ,  $\mathbf{s}_{t,l}$ , and  $\mathbf{p}_{t,l}$  by (10).
6:   end for
7:   Delete the zero elements in  $\mathbf{s}_{t,l}$ , let  $\mathbf{S}_{t,l} = \text{diag}(\mathbf{s}_{t,l})$ , and define the size of  $\mathbf{s}_{t,l}$  as  $R_{t,l}$ .
8:   Delete the corresponding dimensions of  $\mathcal{G}_k$  and let  $\mathcal{X} = \text{STN}(\mathcal{G}, \mathbf{S})$ .
9:   Check the convergence condition:  $\frac{\|\mathcal{X} - \tilde{\mathcal{X}}\|_F}{\|\tilde{\mathcal{X}}\|_F} < 10^{-5}$ .

```

10: end while

Output: \mathcal{G}_k for $\forall k \in \mathbb{K}_N$, and $\mathbf{S}_{t,l}$ and $R_{t,l}$ for $\forall (t, l) \in \mathbb{TL}_N$.

We describe the pseudocode to optimize model (2) in Algorithm 3. Below, we provide the computational complexity and prove a convergence guarantee for the developed algorithm.

Computational complexity. For simplicity, we let the size of the N th-order tensor \mathcal{X} be $I \times I \times \dots \times I$ and the initial rank be (R, R, \dots, R) satisfied $R \leq I$. The computational cost involves updating \mathcal{G} and \mathbf{S} , resulting in costs of $\mathcal{O}(N \sum_{k=2}^N I^k R^{k(N-k)+k-1} + NI^{N-1} R^{2(N-1)} + N^3 IR^N)$ and $\mathcal{O}(N^2 \sum_{k=2}^N I^k R^{k(N-k)+k} + N^4 IR^N + N^2 RI^{2N})$, respectively. In summary, the computational cost at each iteration is $\mathcal{O}(N^2 \sum_{k=2}^N I^k R^{k(N-k)+k} + N^4 IR^N + N^2 RI^{2N})$.

Theorem 1 (Convergence) *The sequence generated by Algorithm 3, denoted by $\{\mathcal{G}^{(s)}, \mathbf{S}^{(s)}\}_{s \in \mathbb{N}}$, converges to a critical point of the optimization problem in (2).*

The numerical convergence is shown in Section 4.3.

3.3 Initialization Scheme

SVDinsTN would encounter high computational cost in the first several iterations if the TN rank $R_{t,l}$ for $\forall (t, l) \in \mathbb{TL}_N$ are initialized with large values. This is due to the utilization of a ‘‘fully-connected’’

topology as a starting point. To solve this issue, we design a novel initialization scheme, which can effectively reduce the initial values of the TN rank.

We first give an upper bound for $R_{t,l}$ in Theorem 2, by which we then design an initialization scheme for both $R_{t,l}$ and diagonal factors $\mathbf{S}_{t,l} \in \mathbb{R}^{R_{t,l} \times R_{t,l}}$ for $\forall (t, l) \in \mathbb{T}\mathbb{L}_N$.

Theorem 2 *Let $\mathcal{X} \in \mathbb{R}^{I_1 \times I_2 \times \dots \times I_N}$ be an N th-order tensor, then there exists an SVDinsTN (1) with the TN rank $R_{t,l} \leq \min(\text{rank}(\mathbf{X}_{(t)}), \text{rank}(\mathbf{X}_{(l)}))$ for $\forall (t, l) \in \mathbb{T}\mathbb{L}_N$.*

Theorem 2 implies that $\min(\text{rank}(\mathbf{X}_{(t)}), \text{rank}(\mathbf{X}_{(l)}))$ can be the initial value of $R_{t,l}$. For real-world data, this value is usually embodied by the rank of mode- (t, l) slices² of \mathcal{X} . Hence, we initialize $R_{t,l}$ and $\mathbf{S}_{t,l}$ by virtue of truncated matrix SVD of mode- (t, l) slices of \mathcal{X} , which consists of the following two steps.

Step 1: We first calculate the mean of all mode- (t, l) slices of \mathcal{X} and denote it by $\mathbf{X}_{t,l}$. Then we perform matrix SVD on $\mathbf{X}_{t,l}$ to obtain $\mathbf{s}_{t,l} \in \mathbb{R}^{\min(I_t, I_l)}$, whose elements are singular values of $\mathbf{X}_{t,l}$.

Step 2: We first let $\mathbf{s}_{t,l} = \text{shrink}(\mathbf{s}_{t,l}, \frac{\gamma \max(\mathbf{s}_{t,l})}{\text{abs}(\mathbf{s}_{t,l}) + \varepsilon})$ and delete zero elements in $\mathbf{s}_{t,l}$. Then we let $\mathbf{S}_{t,l} = \text{diag}(\mathbf{s}_{t,l})$ and define the size of $\mathbf{s}_{t,l}$ as $R_{t,l}$.

In practical applications, the shrink operation in Step 2 effectively reduces the initial value of $R_{t,l}$ by projecting very small singular values in $\mathbf{s}_{t,l}$ to zero. As a result, *the challenge of high computational costs in the first several iterations of SVDinsTN can be effectively addressed* (see Figure 2 for a numerical illustration).

4 Numerical Experiments

In this section, we present numerical experiments on both synthetic and real-world data to evaluate the performance of the proposed SVDinsTN. The primary objective is to validate the following three Claims:

- A: SVDinsTN can reveal a customized TN structure that aligns with the unique structure of a given tensor.
- B: SVDinsTN can greatly reduce time costs while achieving a comparable representation ability to state-of-the-art TN-SS methods. Moreover, SVDinsTN can also surpass existing tensor decomposition methods with pre-defined topologies regarding representation ability.
- C: SVDinsTN can outperform existing tensor decomposition methods in the tensor completion task, highlighting its effectiveness as a valuable tool in applications.

4.1 Experiments for validating Claim A

First of all, we conduct experiments to validate Claim A. Real-world data lacks a true TN structure, and thus we consider synthetic data in this experiment.

Data generation. We first randomly generate $\mathcal{G}_k \in \mathbb{R}^{R_{1,k} \times R_{2,k} \times \dots \times R_{k-1,k} \times I_k \times R_{k,k+1} \times \dots \times R_{k,N}}$ for $\forall k \in \mathbb{K}_N$ and $\mathbf{S}_{t,l} \in \mathbb{R}^{R_{t,l} \times R_{t,l}}$ for $\forall (t, l) \in \mathbb{T}\mathbb{L}_N$, whose elements are taken from a uniform distribution between 0 and 1. Then we obtain the synthetic tensor by $\mathcal{X} = \text{STN}(\mathcal{G}, \mathbf{S})$.

Experiment setting. We test both fourth-order tensors of size $16 \times 18 \times 20 \times 22$ and fifth-order tensors of size $14 \times 16 \times 18 \times 20 \times 22$, and consider five different kinds of TN structures. For each structure, we conduct 100 independent tests and regenerate the synthetic data to ensure reliable and unbiased results. The ability of the proposed SVDinsTN to reveal TN structure is measured by the *success rate* of the output structures, defined as $S_T/T \times 100\%$, where $T = 100$ is the total number of tests and S_T is the number of tests that accurately output the true TN structure. In all tests, the parameter γ is set to 0.0015.

Result analysis. Table 2 presents the *success rate* of the output TN structures obtained by the proposed SVDinsTN in 100 independent tests on fourth-order and fifth-order tensors. It can be observed that the proposed SVDinsTN consistently yields high *success rates* of over 95% in all test cases. Notably, in approximately half of the test cases, the *success rates* reach a perfect score of 100%. Moreover, it is also worth mentioning that in the test on fifth-order tensors, we consider two isomorphic topologies: the “ring” topology and the “five-star” topology. These two topologies are both the “ring” topology (TR

²Mode- (t, l) slices are obtained by fixing all but the mode- t and the mode- l indexes, of a tensor [36].

Table 2: Performance of SVDinsTN on TN structure revealing under 100 independent tests.

True structure (4th-order)					
Success rate	100%	100%	96%	95%	99%
True structure (5th-order)					
Success rate	100%	98%	96%	97%	100%

Table 3: Comparison of the CR (\downarrow) and run time ($\times 1000s$, \downarrow) of different methods on light field data.

Data	Method	RE bound: 0.01		RE bound: 0.05		RE bound: 0.1	
		CR	Time	CR	Time	CR	Time
	TRALS [35]	60.5%	13.54	17.4%	0.471	5.31%	0.118
	FCTNALS [37]	65.1%	13.08	20.9%	0.473	3.93%	0.041
	TNGreedy [11]	26.1%	11.02	6.32%	1.021	2.34%	0.362
	TNGA [13]	27.9%	1014	5.01%	180.3	2.25%	12.52
	TNLS [15]	24.3%	1402	4.26%	63.70	2.16%	24.53
	TNALE [14]	26.3%	144.5	4.52%	18.36	2.26%	3.064
	SVDinsTN	22.4%	0.745	6.92%	0.029	2.66%	0.005
	TRALS [35]	74.7%	10.31	26.9%	3.835	9.15%	0.423
	FCTNALS [37]	73.5%	12.35	20.9%	0.619	3.93%	0.014
	TNGreedy [11]	32.1%	12.53	7.55%	1.366	3.50%	0.481
	TNGA [13]	38.7%	912.9	5.01%	140.2	2.44%	12.52
	TNLS [15]	27.3%	1286	4.73%	75.51	2.15%	5.320
	TNALE [14]	27.6%	266.4	4.52%	25.05	2.10%	3.386
	SVDinsTN	32.0%	1.548	5.64%	0.104	2.76%	0.019
	TRALS [35]	62.8%	17.62	22.6%	1.738	6.00%	0.090
	FCTNALS [37]	69.3%	7.735	20.9%	2.953	3.93%	0.159
	TNGreedy [11]	26.9%	6.676	7.26%	1.259	3.35%	0.488
	TNGA [13]	27.9%	1029	5.01%	170.3	2.85%	14.83
	TNLS [15]	26.4%	992.6	4.99%	119.8	2.57%	19.35
	TNALE [14]	24.7%	239.3	5.77%	19.54	2.90%	5.160
	SVDinsTN	23.5%	1.051	6.42%	0.152	2.83%	0.023

decomposition), but with different permutations: $\mathcal{G}_1 \rightarrow \mathcal{G}_2 \rightarrow \mathcal{G}_3 \rightarrow \mathcal{G}_4 \rightarrow \mathcal{G}_5 \rightarrow \mathcal{G}_1$ and $\mathcal{G}_1 \rightarrow \mathcal{G}_3 \rightarrow \mathcal{G}_5 \rightarrow \mathcal{G}_2 \rightarrow \mathcal{G}_4 \rightarrow \mathcal{G}_1$, respectively. It can be seen that despite the isomorphism, the proposed SVDinsTN can accurately identify the correct permutation for each topology.

4.2 Experiments for Validating Claim B

We conduct experiments to validate Claim B. We consider both real-world data and synthetic data, and use different methods to represent it in this experiment.

Experiment setting. We test three light field data³, named *Bunny*, *Knights*, and *Truck*, which are fifth-order tensors of size $40 \times 60 \times 3 \times 9 \times 9$ (spatial height \times spatial width \times color channel \times vertical grid \times horizontal grid). We employ six representative methods as the compared baselines, including two methods with pre-defined topology: TRALS [35] and FCTNALS [37], and four TN-SS methods: TNGreedy [11], TNGA [13], TNLS [15], and TNALE [14]. We represent the test light field data by different methods and calculate the corresponding *compression ratio* (CR) to achieve a certain *reconstruction error* (RE) bound. The CR is defined as $F_G/F_{\mathcal{X}} \times 100\%$, where F_G is the number of elements of TN cores used to represent a tensor and $F_{\mathcal{X}}$ is the number of total elements of the original tensor. The RE is defined as

³The data is available at <http://lightfield.stanford.edu/lfs.html>.

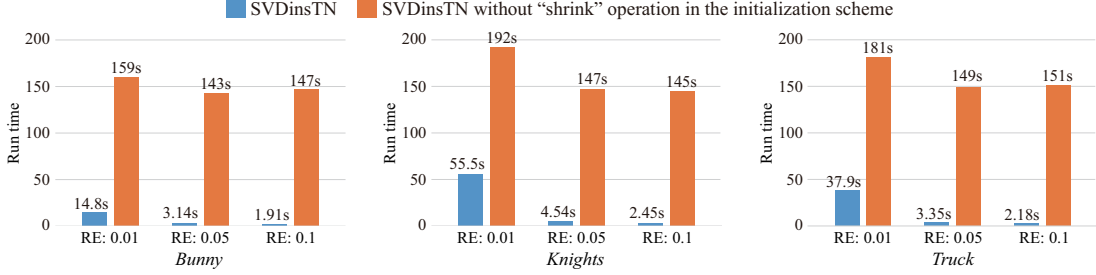


Figure 2: Run time comparison of the first five iterations between SVDinsTN and SVDinsTN without the shrink operation in the initialization scheme.

Table 4: Comparison of the CR (\downarrow) and run time ($\times 1000s$, \downarrow) of different methods when RE bound is 0.01. The result is the average value of 5 independent experiments and “-” indicates “out of memory”.

Method	6th-order		8th-order		10th-order	
	CR	Time	CR	Time	CR	Time
TRALS [35]	1.35%	0.006	0.064%	0.034	-	-
FCTNALS [37]	2.13%	0.002	-	-	-	-
TNGreedy [11]	<u>0.88%</u>	0.167	<u>0.016%</u>	2.625	0.0008%	45.39
TNGA [13]	0.94%	3.825	0.024%	51.40	-	-
TNLS [15]	1.11%	0.673	0.038%	59.83	-	-
TNALE [14]	1.65%	0.201	0.047%	19.96	-	-
SVDinsTN	1.13%	0.002	<u>0.016%</u>	0.017	<u>0.0007%</u>	0.608

$\|\mathcal{X} - \tilde{\mathcal{X}}\|_F / \|\mathcal{X}\|_F$, where \mathcal{X} is the original data and $\tilde{\mathcal{X}}$ is the reconstructed data. In all tests, we select the parameter γ from the interval $[10^{-7}, 10^{-3}]$.

Result analysis. Table 3 reports the *CR* and *run time* of different methods on fifth-order light field data. The results show that the proposed SVDinsTN achieves significantly lower *CR* than TRALS and FCTNALS, which are methods with pre-defined topology. This indicates that SVDinsTN can obtain a more compact structure than the one pre-defined. Besides, while SVDinsTN requires the determination of diagonal matrices alongside TN cores, its iterative process generates progressively simpler structures, enhancing the computational efficiency. Consequently, SVDinsTN demonstrates *faster* performance compared to TRALS and FCTNALS. Furthermore, compared to the TN-SS methods, the proposed SVDinsTN achieves *a substantial speed improvement* while maintaining a comparable level of *CR*. Remarkably, SVDinsTN achieves an acceleration of approximately 100 ~ 1000 times over TNGA, TNLS, and TNALE. This is because TNGreedy, TNGA, TNLS, and TNALE adopt the “sampling-evaluation” framework, necessitating a significant number of repeated structure evaluations. However, SVDinsTN introduces a regularized modeling framework, requiring only a single evaluation.

Impact of the initialization scheme. We analyze the impact of the shrink operation in the initialization scheme under this experimental setting. In Figure 2, we present the *run time* comparison of the initial five iterations between SVDinsTN with the shrink operation and SVDinsTN without the shrink operation in the initialization scheme. As observed, the designed initialization scheme greatly reduces the computational costs in the first several iterations. These findings validate the analysis presented in Section 3.3.

Higher-order cases. We analyze whether the proposed SVDinsTN still performs well on higher-order tensors. We randomly generate 6th-, 8th-, and 10th-order tensors by using the same procedure in Section ???. The size of each tensor mode is randomly selected from $\{5, 6, 7, 8\}$, the edge number of each TN is randomly selected from $\{6, 8, 10\}$, and the rank of each edge is randomly selected from $\{2, 3\}$. For each tensor order, we randomly generate 5 tensors. We compare SVDinsTN and baseline methods in terms of *CR* and *run time* when reaching the RE bound of 0.01, and show the results in Table 4. As observed, SVDinsTN is applicable to higher orders beyond 5, and even up to 10. The behind rational is the truncated SVD used in initialization restricts the initial values of the rank for each edge to a relatively small range, thus improving computational and storage efficiency (see Figure 2). As the iterations progress, the sparsity regularization in the model leads to progressively simpler learned structures, further boosting efficiency.

Table 5: Comparison of MPSNR (\uparrow) and run time (second, \downarrow) of different TC methods on color videos.

Video	FBCP [34]		TMac [26]		TMacTT [3]		TRLRF [30]		TW [25]		SVDinsTN	
	MPSNR	Time	MPSNR	Time	MPSNR	Time	MPSNR	Time	MPSNR	Time	MPSNR	Time
<i>Bunny</i>	28.402	1731	28.211	1203	29.523	453.7	29.163	486.7	30.729	1497	32.401	691.3
<i>News</i>	28.234	1720	27.882	<u>340.4</u>	28.714	535.9	28.857	978.1	30.027	1426	31.643	932.4
<i>Salesman</i>	29.077	1783	28.469	<u>353.6</u>	29.534	656.4	28.288	689.3	30.621	1148	31.684	769.5
<i>Silent</i>	30.126	1453	30.599	<u>316.2</u>	30.647	1305	31.081	453.2	31.731	1232	32.706	532.3

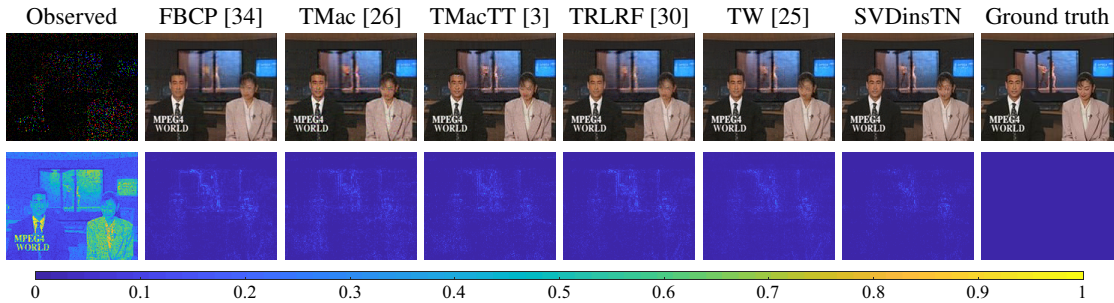


Figure 3: Reconstructed images and residual images obtained by different methods on the 25th frame of *News*. Here the residual image is the average absolute difference between the reconstructed image and the ground truth over R, G, and B channels.

4.3 Experiments for Validating Claim C

We conduct experiments to validate Claim C. We employ the proposed SVDinsTN to a fundamental application, i.e., *tensor completion (TC)*, and compare it with the state-of-the-art tensor decomposition-based TC methods. Given an incomplete observation tensor $\mathcal{F} \in \mathbb{R}^{I_1 \times I_2 \times \dots \times I_N}$ of $\mathcal{X} \in \mathbb{R}^{I_1 \times I_2 \times \dots \times I_N}$, the proposed TC method first updates \mathcal{G} and \mathbf{S} by Algorithm 3, and then updates the target tensor \mathcal{X} as follows: $\mathcal{X} = \mathcal{P}_{\Omega}((\text{STN}(\mathcal{G}, \mathbf{S}) + \rho \hat{\mathcal{X}})/(1 + \rho)) + \mathcal{P}_{\Omega}(\mathcal{F})$, where Ω is the index set of the known elements, $\mathcal{P}_{\Omega}(\mathcal{X})$ is a projection operator which projects the elements in Ω to themselves and all others to zeros, $\hat{\mathcal{X}}$ is the result at the previous iteration, and the initial $\hat{\mathcal{X}}$ is \mathcal{F} .

Experiment setting. We test four color videos⁴, named *Bunny*, *News*, *Salesman*, and *Silent*, which are fourth-order tensors of size $144 \times 176 \times 3 \times 50$ (spatial height \times spatial width \times color channel \times frame). We employ five baseline methods for comparison, named FBCP [34], TMac [26], TMacTT [3], TRLRF [30], and TW [25], respectively. All of them are based on different tensor decompositions. We set the missing ratio (MR) to 90%, which is defined as the ratio of the number of missing elements to the total number of elements. We evaluate the reconstructed quality by *the mean peak signal-to-noise ratio (MPSNR)* computed across all frames. In all tests, the parameter γ is set to 0.0003.

Result analysis. Table 5 reports *MPSNR* and *run time* obtained by different TC methods. As observed, the proposed SVDinsTN consistently achieves the highest *MPSNR* values among all utilized TC methods across all test color videos. Besides, SVDinsTN exhibits comparable *run time* to the baseline methods. Figure 3 displays the reconstructed images and their corresponding residual images at the 25th frame of *News*. We observe that the proposed SVDinsTN outperforms the baseline methods in terms of visual quality, particularly with respect to background cleanliness and local details (e.g., “dancer”) recovery.

Numerical convergence. In Theorem 1, we provide a *theoretical* convergence guarantee for the proposed method. Here, we *numerically* verify the convergence. Figure 4 presents the relative change in the reconstructed color videos at each iteration compared to their respective previous iterations. We observe that the values of the relative change achieved by the proposed method decrease and gradually tend to zero as the number of iterations increases. This justifies the numerical convergence of the proposed method.

⁴The data is available at <http://trace.eas.asu.edu/yuv/>.

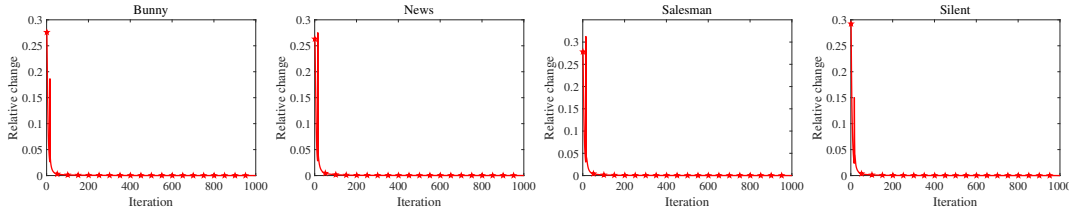


Figure 4: Relative change curves with respect to the iteration number on four test color videos. Here the relative change is defined as $\|\mathcal{X}^c - \mathcal{X}^p\|_F / \|\mathcal{X}^p\|_F$, and \mathcal{X}^c and \mathcal{X}^p are the results of the current iteration and its previous iteration.

5 Conclusion

Summary. We propose a novel TN paradigm, called SVDinsTN, which enables us to solve the challenging TN-SS problem from a regularized modeling perspective. This perspective renders our model highly amenable to easy solutions, allowing us to leverage well-established optimization algorithms for tackling the regularized model. As a result, the proposed method achieves approximately 100 ~ 1000 times acceleration compared to the state-of-the-art TN-SS methods with a comparable representation ability. Additionally, SVDinsTN demonstrates its effectiveness as a valuable tool in practical applications.

Limitations. In existing research on the TN-SS problem, two challenging issues remain open. One is the computationally consuming issue, and the other is the theoretical guarantee of the optimal TN structure. SVDinsTN provides a new regularized modeling perspective to fundamentally address the computationally consuming issue and proves theorems regarding the upper bound of the TN rank and the convergence. However, the theoretical guarantee of the optimal TN structure is still an open problem. Solving this issue will be the direction of our future work.

Acknowledgments

We would like to express our gratitude to Guillaume Rabusseau for his valuable assistance in correcting the experimental results of “TN-Greedy”.

References

- [1] A. Anandkumar, R. Ge, D. Hsu, S. M. Kakade, and M. Telgarsky, “Tensor decompositions for learning latent variable models,” *The Journal of Machine Learning Research*, vol. 15, no. 1, p. 2773–2832, 2014.
- [2] H. Attouch, J. Bolte, P. Redont, and A. Soubeyran, “Proximal alternating minimization and projection methods for nonconvex problems: An approach based on the Kurdyka-Łojasiewicz inequality,” *Mathematics of Operations Research*, vol. 35, no. 2, pp. 438–457, 2010.
- [3] J. A. Bengua, H. N. Phien, H. D. Tuan, and M. N. Do, “Efficient tensor completion for color image and video recovery: Low-rank tensor train,” *IEEE Transactions on Image Processing*, vol. 26, no. 5, pp. 2466–2479, 2017.
- [4] A. Cichocki, N. Lee, I. Oseledets, A.-H. Phan, Q. Zhao, and D. P. Mandic, “Tensor networks for dimensionality reduction and large-scale optimization: Part 1 low-rank tensor decompositions,” *Foundations and Trends® in Machine Learning*, vol. 9, no. 4-5, pp. 249–429, 2016.
- [5] A. Cichocki, D. Mandic, L. De Lathauwer, G. Zhou, Q. Zhao, C. Caiafa, and H. A. PHAN, “Tensor decompositions for signal processing applications: From two-way to multiway component analysis,” *IEEE Signal Processing Magazine*, vol. 32, no. 2, pp. 145–163, 2015.
- [6] D. Gabay and B. Mercier, “A dual algorithm for the solution of nonlinear variational problems via finite element approximation,” *Computers and Mathematics with Applications*, vol. 2, no. 1, pp. 17–40, 1976.
- [7] S. Garnerone, T. R. de Oliveira, and P. Zanardi, “Typicality in random matrix product states,” *Physical Review A*, vol. 81, p. 032336, 2010.
- [8] M. Ghadiri, M. Fahrback, G. Fu, and V. Mirrokni, “Approximately optimal core shapes for tensor decompositions,” *arXiv preprint arXiv:2302.03886*, 2023.
- [9] I. Glasser, R. Sweke, N. Pancotti, J. Eisert, and J. I. Cirac, “Expressive power of tensor-network factorizations for probabilistic modeling,” in *Advances in Neural Information Processing Systems*, vol. 32, 2019.

- [10] G. H. Golub, P. C. Hansen, and D. P. O’Leary, “Tikhonov regularization and total least squares,” *SIAM journal on matrix analysis and applications*, vol. 21, no. 1, pp. 185–194, 1999.
- [11] M. Hashemizadeh, M. Liu, J. Miller, and G. Rabusseau, “Adaptive learning of tensor network structures,” *arXiv preprint arXiv:2008.05437*, 2020.
- [12] C. J. Hillar and L.-H. Lim, “Most tensor problems are NP-hard,” *Journal of the ACM*, vol. 60, no. 6, pp. 1–39, 2013.
- [13] C. Li and Z. Sun, “Evolutionary topology search for tensor network decomposition,” in *Proceedings of the 37th International Conference on Machine Learning*, vol. 119, 2020, pp. 5947–5957.
- [14] C. Li, J. Zeng, C. Li, C. Caiafa, and Q. Zhao, “Alternating local enumeration (tnale): Solving tensor network structure search with fewer evaluations,” in *Proceedings of the 40th International Conference on Machine Learning*, 2023.
- [15] C. Li, J. Zeng, Z. Tao, and Q. Zhao, “Permutation search of tensor network structures via local sampling,” in *Proceedings of the 39th International Conference on Machine Learning*, vol. 162, 2022, pp. 13 106–13 124.
- [16] C. Li and Q. Zhao, “Is rank minimization of the essence to learn tensor network structure?” in *Second Workshop on Quantum Tensor Networks in Machine Learning (QTNML), Neurips*, 2021.
- [17] N. Li, Y. Pan, Y. Chen, Z. Ding, D. Zhao, and Z. Xu, “Heuristic rank selection with progressively searching tensor ring network,” *Complex & Intelligent Systems*, vol. 8, no. 2, pp. 771–785, 2022.
- [18] Y. Liu, Y. Lu, W. Ou, Z. Long, and C. Zhu, “Adaptively topological tensor network for multi-view subspace clustering,” *arXiv preprint arXiv:2305.00716*, 2023.
- [19] Y. Luo, X.-L. Zhao, D. Meng, and T.-X. Jiang, “Hlrf: Hierarchical low-rank tensor factorization for inverse problems in multi-dimensional imaging,” in *2022 IEEE/CVF Conference on Computer Vision and Pattern Recognition (CVPR)*, 2022, pp. 19 281–19 290.
- [20] C. Nie, H. Wang, and L. Tian, “Adaptive tensor networks decomposition,” in *British Machine Vision Conference*, 2021.
- [21] R. Orús, “A practical introduction to tensor networks: Matrix product states and projected entangled pair states,” *Annals of Physics*, vol. 349, pp. 117–158, 2014.
- [22] I. V. Oseledets, “Tensor-train decomposition,” *SIAM Journal on Scientific Computing*, vol. 33, no. 5, pp. 2295–2317, 2011.
- [23] P. Rai, Y. Wang, S. Guo, G. Chen, D. Dunson, and L. Carin, “Scalable bayesian low-rank decomposition of incomplete multiway tensors,” in *Proceedings of the 31st International Conference on International Conference on Machine Learning*, vol. 32, 2014, p. II–1800–II–1808.
- [24] F. Sedighin, A. Cichocki, and A.-H. Phan, “Adaptive rank selection for tensor ring decomposition,” *IEEE Journal of Selected Topics in Signal Processing*, vol. 15, no. 3, pp. 454–463, 2021.
- [25] Z.-C. Wu, T.-Z. Huang, L.-J. Deng, H.-X. Dou, and D. Meng, “Tensor wheel decomposition and its tensor completion application,” in *Advances in Neural Information Processing Systems*, vol. 35, 2022, pp. 27 008–27 020.
- [26] Y. Xu, R. Hao, W. Yin, and Z. Su, “Parallel matrix factorization for low-rank tensor completion,” *Inverse Problems and Imaging*, vol. 9, no. 2, pp. 601–624, 2015.
- [27] R. Yamamoto, H. Hontani, A. Imakura, and T. Yokota, “Fast algorithm for low-rank tensor completion in delay-embedded space,” in *2022 IEEE/CVF Conference on Computer Vision and Pattern Recognition (CVPR)*, 2022, pp. 2048–2056.
- [28] K. Ye and L.-H. Lim, “Tensor network ranks,” *arXiv preprint arXiv:1801.02662*, 2018.
- [29] L. Yuan, J. Cao, X. Zhao, Q. Wu, and Q. Zhao, “Higher-dimension tensor completion via low-rank tensor ring decomposition,” in *Asia-Pacific Signal and Information Processing Association Annual Summit and Conference*, 2018, pp. 1071–1076.
- [30] L. Yuan, C. Li, D. Mandic, J. Cao, and Q. Zhao, “Tensor ring decomposition with rank minimization on latent space: An efficient approach for tensor completion,” in *Proceedings of the AAAI Conference on Artificial Intelligence*, vol. 33, no. 1, 2019, pp. 9151–9158.
- [31] L. Yuan, Q. Zhao, L. Gui, and J. Cao, “High-order tensor completion via gradient-based optimization under tensor train format,” *Signal Processing: Image Communication*, vol. 73, pp. 53–61, 2019.
- [32] S. Zhang, L. Wang, L. Zhang, and H. Huang, “Learning tensor low-rank prior for hyperspectral image reconstruction,” in *2021 IEEE/CVF Conference on Computer Vision and Pattern Recognition (CVPR)*, 2021, pp. 12 001–12 010.
- [33] X. Zhang, X. Yuan, and L. Carin, “Nonlocal low-rank tensor factor analysis for image restoration,” in *2018 IEEE/CVF Conference on Computer Vision and Pattern Recognition*, 2018, pp. 8232–8241.

- [34] Q. Zhao, L. Zhang, and A. Cichocki, “Bayesian CP factorization of incomplete tensors with automatic rank determination,” *IEEE Transactions on Pattern Analysis and Machine Intelligence*, vol. 37, no. 9, pp. 1751–1763, 2015.
- [35] Q. Zhao, G. Zhou, S. Xie, L. Zhang, and A. Cichocki, “Tensor ring decomposition,” *arXiv preprint arXiv:1606.05535*, 2016.
- [36] Y.-B. Zheng, T.-Z. Huang, X.-L. Zhao, T.-X. Jiang, T.-Y. Ji, and T.-H. Ma, “Tensor N-tubal rank and its convex relaxation for low-rank tensor recovery,” *Information Sciences*, vol. 532, pp. 170–189, 2020.
- [37] Y.-B. Zheng, T.-Z. Huang, X.-L. Zhao, Q. Zhao, and T.-X. Jiang, “Fully-connected tensor network decomposition and its application to higher-order tensor completion,” in *Proceedings of the AAAI Conference on Artificial Intelligence*, vol. 35, no. 12, 2021, pp. 11 071–11 078.